ACS APPLIED MATERIALS & INTERFACES

Research Article

www.acsami.org

Response Characteristics of Bisphenols on a Metal–Organic Framework-Based Tyrosinase Nanosensor

Xianbo Lu,*[,†,∥] Xue Wang,[†,‡,∥] Lidong Wu,[§] Lingxia Wu,[†] Dhanjai,[†] Lei Fu,[†] Yuan Gao,[†] and Jiping Chen*[,†]

[†]Key Laboratory of Separation Science for Analytical Chemistry, Dalian Institute of Chemical Physics, Chinese Academy of Sciences, Dalian 116023, China

[‡]School of Food and Environment, Dalian University of Technology, Panjin 124221, China

[§]Chinese Academy of Fishery Sciences, Beijing 100141, China

ABSTRACT: Bisphenols (BPs), which have more than ten kinds of structural analogues, are emerging as the most important endocrine disrupting chemicals that adversely affect human health and aquatic life. A tyrosinase nanosensor based on metal–organic frameworks (MOFs) and chitosan was developed to investigate the electrochemical response characteristics and mechanisms of nine kinds of BPs for the first time. The developed tyrosinase nanosensor showed a sensitive response to bisphenol A, bisphenol F, bisphenol E, bisphenol B, and bisphenol Z, and the responsive sensitivities were highly dependent on their respective log K_{ow} values. However, the nanosensor showed no response to bisphenol S (BPS), bisphenol AP (BPAP), bisphenol AF (BPAF), or tetrabromobisphenol A, although BPS, BPAP, and BPAF have structures similar to those of the responsive BPs. The obtained results reveal that the electrochemical response of different BPs is affected not only by the molecular structure, especially the available ortho positions of phenolic hydroxyl groups, but also by the substituent group properties (electron acceptor or electron donor) on the bisphenol framework. The electronic cloud distribution of the phenolic hydroxyl groups, which is affected by the substituent group, determines whether the available ortho positions of phenolic hydroxyl groups can be oxidized by the tyrosinase biosensor. These response mechanisms are very significant as they can be used for predicting the response characteristics of many BPs and their various derivatives and metabolites on biosensors. The unexpected anti-interference ability of the biosensor to nine heavy metal ions was also discovered and discussed. The MOF-chitosan nanocomposite proves to be a promising sensing platform for the construction of diverse biosensors for selective detection of targets even in the presence of a high concentration of heavy metal ions.

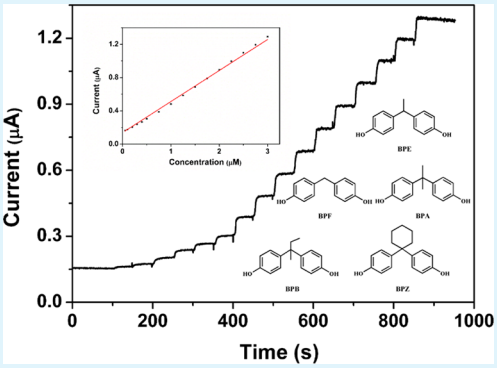

KEYWORDS: *bisphenols, heavy metal ions, electrochemical response mechanism, metal–organic frameworks, tyrosinase biosensor*

1. INTRODUCTION

Bisphenols (BPs) (Figure 1) structurally consist of two phenolic rings joined through a bridging carbon or other chemical groups, including many kinds of analogues such as 2,2′-bis(4-hydroxyphenyl)propane (BPA), 2,2′-bis(4-hydroxyphenyl)butane (BPB), 4,4′-ethylidenebisphenol (BPE), 4,4′-dihydroxydiphenylmethane (BPF), 1,1′-bis(4-hydroxyphenyl)-cyclohexane (BPZ), bis(4-hydroxyphenyl)sulfone (BPS), 1,1′-bis(4-hydroxyphenyl)-1-phenyl-ethane (BPAP), 2,2′-bis(4-hydroxyphenyl)hexafluoropropane (BPAF), tetrachlorobisphenol A (TCBPA), and tetrabromobisphenol A (TBBPA). Among all of the analogues, BPA has been studied extensively for its ubiquity in our daily commodities. BPA is a high production volume chemical used as an intermediate in the synthesis of polycarbonates, epoxy resins, and thermal papers, which are common ingredients of daily use products as food contact materials.[1] BPA (usually leaching from consumer products to the surroundings) is known to be one of the most ubiquitous endocrine disrupting chemicals. In many countries, BPA has been banned in the production of baby bottles and formula packaging due to its endocrine disrupting activity and toxic effects.[2−4] Therefore, many of structural analogues of BPA such as BPS and BPE were developed as alternatives to BPA for use in industrial production.[5] Unfortunately, recent studies indicated that these BPA analogues also had estrogenic activity and mutagenicity similar to BPA, which may cause serious adverse human health risks.[6]

Conventional analytical methods for BPs are usually based on high-performance liquid chromatography-tandem mass spectrometry[7] and gas chromatography–mass spectrometry.[8,9] These analytical methods require expensive equipment, highly trained technicians, and time-consuming sample pretreatment

Received: April 27, 2016
Accepted: June 9, 2016
Published: June 9, 2016

DOI: 10.1021/acsami.6b05008
ACS Appl. Mater. Interfaces 2016, 8, 16533−16539

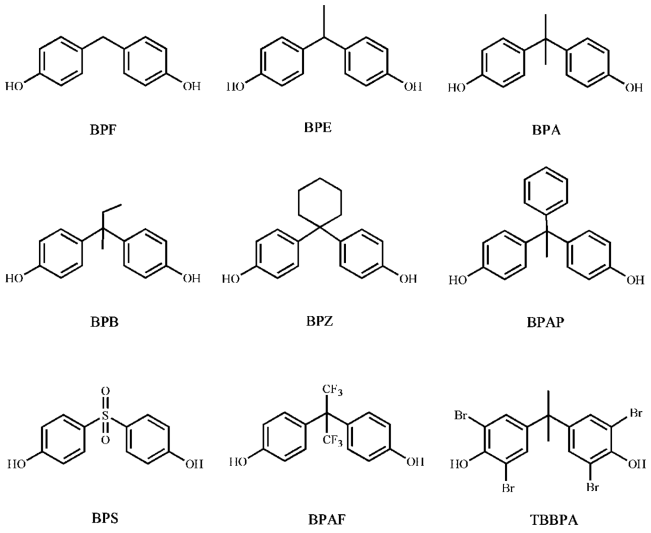

Figure 1. Molecular structures of BPA and its structural analogues.

processes. Tyrosinase as an ortho-hydroxylation oxidase possesses catalytic bioactivity for monophenol and *o*-diphenol. Tyrosinase can oxidize BPA to corresponding *o*-diphenols and *o*-quinones, which further can be reduced at the electrode surface. The reduction current is proportional to the concentration of BPA. On the basis of this principle, some attempts have been made to develop electrochemical tyrosinase biosensors for the rapid determination of BPA.[10] Compared with conventional instrument-based methods, electrochemical tyrosinase biosensors provide a more rapid, convenient, and economic method for the determination of BPA and its analogues. To date, almost all of the present biosensing methods focus on BPA only, and no studies relate to the structural analogues despite their similar estrogenic activity to BPA.[11−14] Until now, there has been no information about the response characteristics of BPA analogues on electrochemical tyrosinase biosensors.

Metal−organic frameworks, as an emerging class of nanoporous materials, are constructed by metal-containing nodes connected by organic bridges.[15] Due to their unique properties, such as extremely high surface area (usually >1000 m^2 g^{-1}) and structural and functional tunability, research on MOFs has become one of the most vigorously developing fields in chemistry.[16−20] Recently, development of new strategies for enzyme immobilization on MOFs with interesting results shows great promise in biosensing applications.[21,22] Ma et al.[22] explored zeolitic imidazolate frameworks (ZIFs) as the matrix for constructing dehydrogenase-based glucose biosensors, and ZIF-70 showed excellent adsorption capacities toward dehydrogenase immobilization with excellent analytical properties. In our previous study,[23] we exploited the advantageous characteristics of metal−organic frameworks for preparation of a tyrosinase-based biosensor for BPA detection. Copper-centered MOF (abbreviated as CuMOF), consisting of a copper ion center with two organic ligands, was explored for fabricating a tyrosinase biosensor to improve the biosensing performance because this nanoporous nanomaterial with a high surface area is advantageous not only for tyrosinase immobilization but also for BPA preconcentrate on the biosensor surface through a $\pi-\pi$ stacking interaction between the aromatic rings of BPA and the organic ligands of MOFs.

Chitosan is a natural biopolymer with an excellent film-forming ability. Owing to its biocompatible, nontoxic, and high mechanical strength properties, chitosan is usually used to immobilize enzymes for fabricating biosensors with good stability.[24−26] In this study, chitosan was used to immobilize CuMOF and tyrosinase to fabricate a nanobiosensor. The electrochemical response characteristics and mechanisms of nine commonly used BPs on the tyrosinase biosensing platform was investigated in detail for the first time. Because environmental water samples are extremely complex, usually containing heavy metal ions, the response behaviors of the CuMOF-based tyrosinase biosensor for nine heavy metal ions (Hg^{2+}, Pd^{2+}, Cu^{2+}, Fe^{2+}, Co^{2+}, Ba^{2+}, Zn^{2+}, Cd^{2+}, and Ni^{2+}) were evaluated, and an unexpected excellent anti-interference ability for high concentrations of heavy metal ions was discovered. As far as we know, this is the first systematic investigation on electrochemical response characteristics of different BPs and heavy metal ions on fabricated tyrosinase biosensors. On the basis of the experimental results and discoveries, the potential promising applications of the fabricated tyrosinase biosensor and the CuMOF-based biosensing platform are proposed.

2. EXPERIMENTAL SECTION

2.1. Reagents and Materials. Bisphenol A (BPA), bisphenol B (BPB), bisphenol S (BPS), bisphenol F (BPF), bisphenol E (BPE), bisphenol Z (BPZ), bisphenol AF (BPAF), bisphenol AP (BPAP), and tetrabromide bisphenol A (TBBPA) were purchased from J&K Chemical Ltd. (Beijing, China). Triethylenediamine, chitosan (>75% deacetylated), and tyrosinase (>1000 units mg^{-1}) were provided by Sigma-Aldrich (Beijing, China). 1,4-benzenedicarboxylic acid was supplied by Aladdin (Shanghai, China). $Cu(NO_3)_2{\cdot}3H_2O$, $Cd(NO_3)_2{\cdot}4H_2O$, $Zn(NO_3)_2{\cdot}6H_2O$, $Ba(NO_3)_2$, $Ni(NO_3)_2{\cdot}6H_2O$, $Pb(NO_3)_2$, $CoCl_2{\cdot}6H_2O$, $HgCl_2$, and $FeSO_4{\cdot}7H_2O$ were all analytical grade. The phosphate buffer solutions (PBS, 50 mM, pH 7.0) were prepared from K_2HPO_4 and KH_2PO_4. Millipore-Q water (>18.2 MΩ cm) was used for the preparation of buffer solutions.

2.2. Synthesis of CuMOF. CuMOF was synthesized directly by a solvothermal method according to our previously reported method.[27] Briefly, copper nitrate trihydrate (0.493 g), triethylenediamine (0.32 g), and 1,4-benzenedicarboxylic acid (0.453 g) were mixed with 100 mL of DMF and homogenized by sonication. The mixture was transferred into an autoclave and subsequently heated at 120 °C for 36 h. A blue color crystalline powder was obtained. The resulting product was filtered, washed several times with DMF, and dried under vacuum overnight.

2.3. Fabrication of the CuMOF-Based Biosensor. Prior to the fabrication of the biosensor, the bare glassy carbon electrode (GCE) was mechanically polished on a micro cloth to obtain a mirror-like surface using 1.0, 0.3, and 0.05 μm alumina slurries. Then, the GCE was rinsed with water and ultrasonicated in ethanol and water successively. The composition for the preparation of the CuMOF-Tyr-Chit/GCE biosensor was optimized, and the final concentrations of CuMOF, tyrosinase, and chitosan were 0.5 mg mL^{-1}, 2.5 mg mL^{-1}, and 1.5 mg mL^{-1}, respectively. The preparation process followed these steps: first, 1.0 mg of CuMOF was dispersed into 1.0 mL water to form a homogeneous suspension under ultrasonication for 0.5 h. Then, 20 μL of a CuMOF suspension (1.0 mg mL^{-1}) and 10 μL of a tyrosinase solution (10 mg mL^{-1}) were mixed and shaken for 1 h, and 10 μL of a chitosan solution (6.0 mg mL^{-1}) was added into the above solution. Finally, 4 μL of the CuMOF-Tyr-Chit composite was dropped on the surface of the bare GCE and dried at room temperature.

2.4. Electrochemical Response of BPs and Heavy Metal Ions on the Biosensor. The electrochemical response characteristics of BPs on the CuMOF-Tyr-Chit biosensor were investigated by cyclic voltammetry and amperometry in PBS (50 mM, pH 7.0). For the

DOI: 10.1021/acsami.6b05008
ACS Appl. Mater. Interfaces 2016, 8, 16533−16539

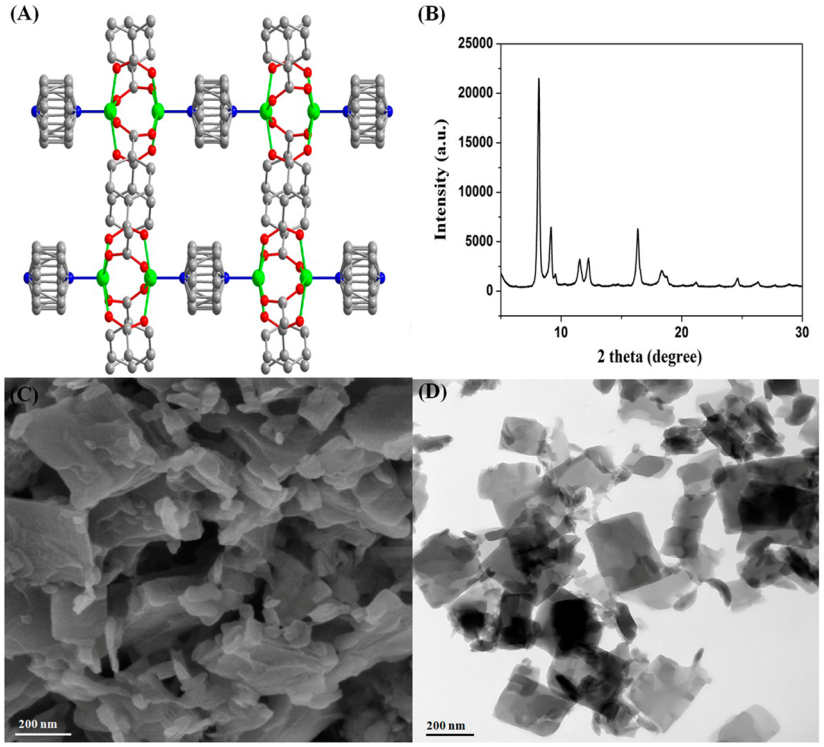

Figure 2. (A) Chemical structure of CuMOF: Cu (green), O (red), N (blue), and C (gray). For clarity, the H atoms are omitted. (B) XRD pattern of CuMOF. (C) and (D) are SEM and TEM images of CuMOF, respectively.

amperometric determination, BPs were added into the PBS successively under stirring at an applied optimum potential of −0.1 V.

The effect of heavy metal ions on the biosensor was evaluated by amperometry based on the change in the biosensor sensitivity. The sensitivity of the biosensor for catechol (the natural substrate of tyrosinase) was regarded as the original sensitivity (S_o). Then, the biosensor was immersed in a heavy metal ion buffer solution for 0.5 h, and the remaining sensitivity (S_r) of the biosensor for catechol was determined again using amperometry. The remaining percentage of sensitivity (S_p, i.e., $S_r/S_o \times 100\%$) was used as an index for the evaluation of the heavy metal ion toward the biosensor. For every heavy metal ion (Hg^{2+}, Pd^{2+}, Cu^{2+}, Fe^{2+}, Co^{2+}, Ba^{2+}, Zn^{2+}, Cd^{2+}, and Ni^{2+}), the average S_p of three determinations was used.

3. RESULTS AND DISCUSSION

3.1. Characterization of CuMOF. CuMOF was synthesized using triethylenediamine, 1,4-benzenedicarboxylic acid, and copper nitrate trihydrate as precursors by a solvothermal method. It can be seen that CuMOF was synthesized under the conditions of high metal ion concentration and high temperature for a long time (at 120 °C for 36 h). In the structure of CuMOF, each paddle-wheel secondary building unit is linked by 1,4-benzenedicarboxylic acid within the layer to form a two-dimensional (2D) net parallel to the *XY* plane, which is further connected by triethylenediamine molecules to produce a robust three-dimensional (3D) framework. The chemical bonds of the central metal ion Cu(II) are saturated, and the framework is not easily damaged by other metal ions. The chemical structure of CuMOF is illustrated in Figure 2A. CuMOF possesses a paddle-wheel structure in which Cu units are bridged by 1,4-benzenedicarboxylic acid linkers to form a 2D square-grid net. The triethylenediamine pillars extend the 2D layers into a 3D porous structure. The synthesized CuMOF was characterized by X-ray diffraction (XRD), scanning electron microscopy (SEM), transmission electron microscopy (TEM), and nitrogen adsorption−desorption measurements.

The crystallographic structure of CuMOF was confirmed by XRD analysis. Figure 2B displays the XRD data of CuMOF. The whole XRD patterns of CuMOF were in good agreement with those in a previous report,[27] which demonstrated that CuMOF was successfully obtained. The SEM and TEM images (Figures 2C and D, respectively) show that CuMOF is highly crystalline, which is consistent with the XRD analysis results. The images of CuMOF exhibit a high-quality brick-like morphology of approximately 20−250 nm. CuMOF possesses a surface area of 1006 $m^2\ g^{-1}$ with a pore size distribution peak at ∼4.9 Å according to the nitrogen adsorption−desorption measurements. As an enzyme immobilization matrix, the large surface area can promote enzyme adsorption on the surface of the modified electrode,[23] and the increased amount of enzyme loading can improve the analytical performance of the biosensor. Additionally, it should be noted that some small molecules (such as H^+) in the PBS solution can transfer and diffuse through the porous 3D structure of CuMOF. These 3D regular nanoporous structures and interconnected channels allow fast ion transfer in the supporting electrolyte, which is very important for enhancing the transducing ability of the obtained electrochemical biosensor.

3.2. Electrochemical Response Characteristics of BPs on the Tyrosinase Biosensor. Besides BPA, a group of chemicals structurally similar to BPA, including BPF, BPE, BPB, BPZ, BPAP, BPS, BPAF, TCBPA, and TBBPA, have been used as substitutes for BPA in industrial plastic production. These chemicals gradually become an emerging class of endocrine disruptors with high estrogenic effects. In the fabricated CuMOF-Tyr-Chit biosensor, the current response for BPs was investigated by cyclic voltammetry and amperometry. With BPE as an example, the amperometric

DOI: 10.1021/acsami.6b05008
ACS Appl. Mater. Interfaces 2016, 8, 16533−16539

response of the biosensor upon successive addition of different concentrations of BPE into PBS (50 mM, pH 7.0) under stirring at an applied potential of −0.1 V is shown in Figure 3.

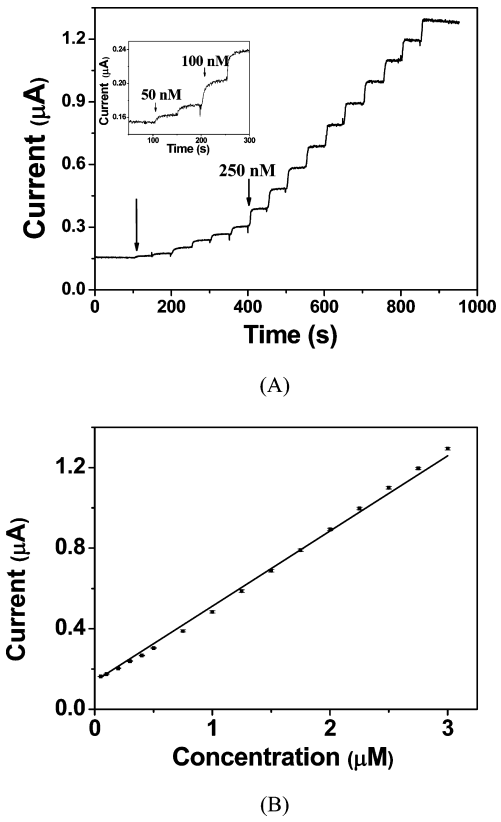

Figure 3. (A) Amperometric current−time response curve of BPE on the CuMOF-Tyr-Chit/GCE biosensor. Inset: amplified response curve. (B) Linear calibration curve for BPE concentrations from 50 nM to 3 μM.

After the addition of BPE, there is an obvious increase in the response current. The current change is caused by the bioelectrocatalysis reaction of the biosensor for BPE. The CuMOF-based biosensor showed a wide linear range for BPE from 5.0×10^{-8} to 3.0×10^{-6} mol L^{-1}. The sensitivity was as high as 5.51 A M^{-1} cm^{-2}, and the limit of detection (LOD) was as low as 15 nmol L^{-1} (S/N = 3). The repeatability of the biosensor was also evaluated by amperometry. The relative standard deviation of the biosensor for 10 successive detections of BPE was about 6.1%, demonstrating good repeatability. In previous studies, tyrosinase-based electrochemical biosensors were constructed to detect BPA with good analytical performance. The mechanism for the enzymatic reaction on the tyrosinase biosensor has been discussed in detail.[28] The reaction equations are as follows:

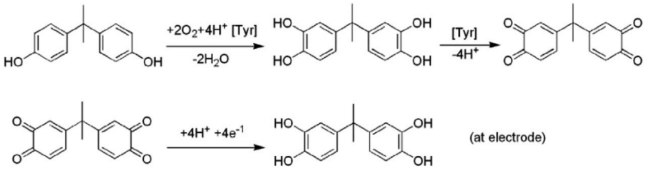

From the reaction equations, we clearly know that the current response of biosensor for the BPs is from the reduction current of *o*-diquinone into *o*-dihydroxybenzene at the electrode surface.

Table 1 summarizes the linear range, sensitivity, and LOD of the developed biosensor for BPE, BPF, BPA, BPB, and BPZ. From Table 1, it can be found that the biosensor exhibited good current response for BPE, BPF, BPA, BPB, and BPZ with sensitivities of 5.51, 4.66, 3.17, 1.34, and 1.13 A M^{-1} cm^{-2}, respectively. The high sensitivity of CuMOF-Tyr-Chit/GCE to BPs was conducive to investigate the response mechanism. This high sensitivity was attributed to the following reasons. First, CuMOF possesses an extremely large specific surface area (>1000 m^2 g^{-1}), which was favorable for enzyme immobilization and BPs absorption and thus improved the sensitivity of the biosensor. Second, there were strong $\pi-\pi$ interactions between the aromatic rings of guest molecules and organic ligands of MOFs.[29,30] CuMOF could preconcentrate the reactive BPs on the biosensor surface through $\pi-\pi$ stacking interactions between the two aromatic rings of the BPs and the benzenedicarboxylate ligands of CuMOF, which further improved the sensitivity of the biosensor.

Generally speaking, the fabricated biosensor showed high sensitivity for five BPs along with a wide linear range from 5.0×10^{-8} to 8.0×10^{-6} mol L^{-1} and a low detection limit from 13 to 56 nM. It is noteworthy that the sensitivity of the biosensor follows the order BPE > BPF > BPA > BPB > BPZ in the range 5.51 to 1.13 A M^{-1} cm^{-2}. It is well-known that the electrochemical response characteristics of different chemicals on the same electrode will be affected mainly by the physical and chemical properties of the analytes. The five BPs have molecular structures that are quite similar (Figure 1) and almost the same oxidation−reduction potentials on the tyrosinase biosensor. It is interesting to find a remarkable correlation between the sensitivity values and the logarithms of the *n*-octanol/water partition coefficients (log K_{ow}) of responsive BPs with a correlation coefficient of 0.94, as shown in Figure 4. When log K_{ow}(BPF) = 2.764, the sensitivity of BPF is 4.66 A M^{-1} cm^{-2}, and when log K_{ow}(BPZ) = 4.870, the sensitivity of BPZ is 1.13 A M^{-1} cm^{-2}. The sensitivity decreases as the value of log K_{ow} increases. This result indicated that the sensitivity for BPs was influenced by the log K_{ow} of the BPs. It is reasonable considering that the log K_{ow} value plays a key role in affecting the diffusion and mass transfer of BPs in the interface between the electrode surface and aqueous phase. In fact, the reasons for the specific response of different BPs on the biosensor (e.g., detection limit, sensitivity) are quite complicated and depend on more parameters than log K_{ow}. For example, the incorporation efficiency of different BPs onto the CuMOF surface or substrate binding of tyrosinase also play an important role. On the basis of the previously published literature reports[29,30] and the chemical structure of BPs and CuMOF, we believe there are strong $\pi-\pi$ stacking interactions between BPs and CuMOF. The enrichment of the BPs onto the CuMOF surface resulted in the increased detection sensitivity of the biosensor.

In addition, BPAP, BPS, BPAF, and TBBPA were also detected by the CuMOF-based tyrosinase biosensor. Figure 5 shows the cyclic voltammograms of the biosensor for the responsive (BPF, BPE) and unresponsive BPs (BPS and TBBPA). The biosensor showed obvious electrochemical responses after the addition of 3 μM BPF (curve a, black line) or 3 μM BPE (curve b, black line), as shown in Figure 5A. However, after the addition of 3 μM TBBPA (Figure 5C) or 3 μM BPS (Figure 5D), the biosensor showed no response.

DOI: 10.1021/acsami.6b05008
ACS Appl. Mater. Interfaces 2016, 8, 16533−16539

Table 1. Response Characteristics of the CuMOF-Tyr-Chit/GCE Biosensor to Bisphenols

BPs	linear range (M)	correlation coefficient	sensitivity (A M^{-1} cm^{-2})	detection limit (nM)	log K_{ow} [a]
BPE	5.0×10^{-8} to 3.0×10^{-6}	0.9994	5.51	15	3.230
BPF	5.0×10^{-8} to 3.0×10^{-6}	0.9997	4.66	16	2.764
BPA	5.0×10^{-8} to 3.0×10^{-6}	0.9998	3.17	13	3.641
BPB	1.25×10^{-7} to 8.0×10^{-6}	0.9994	1.34	56	4.150
BPZ	2.5×10^{-7} to 5.0×10^{-6}	0.9986	1.13	33	4.870

[a]Software-calculated value from the SciFinder Scholar Database.

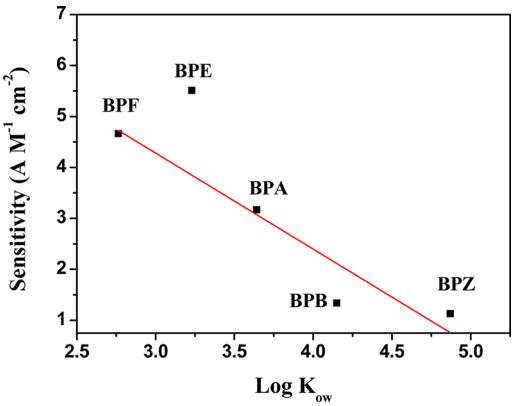

Figure 4. Correlation between the sensitivity values and the log K_{ow} of the BPs.

Tyrosinase is an ortho-hydroxylation oxidase which has catalytic bioactivity for monophenol and *o*-diphenol.[31] In accordance with our expectations, neither TBBPA nor TCBPA showed a response on the biosensor, as the ortho positions of their phenolic hydroxyl groups are occupied by halogen substituents, and TBBPA and TCBPA have no available ortho position in their phenolic hydroxyl groups for ortho-hydroxylation by tyrosinase. It was not our expectation that BPAP, BPS, and BPAF also did not exhibit a response on the biosensor even though they have two available monophenol units in their respective molecules, and the ortho positions of phenolic hydroxyl groups are available. The log K_{ow} values of BPS and BPAF are 2.139 and 3.975, respectively, which are less than the log K_{ow} of BPZ. By further comparison, we can find the real difference between the five responsive BPs (BPF, BPE, BPA, BPB, and BPZ) and the three unresponsive BPs (BPAP, BPS, and BPAF). The five responsive BPs have several methyl or methylene groups on the bisphenol framework (4,4′ position), and these methyl or methylene groups are strong electron donors. Therefore, these five BPs can be ortho-hydroxylated by tyrosinase. However, the sulfonyl group of BPS and the trifluoromethyl group of BPAF are strong electron acceptors, and the phenyl group of BPAP (4,4′ position) is a weak electron acceptor, which can inhibit enzymatic oxidation of BPs to the corresponding *o*-quinones. In sum, the

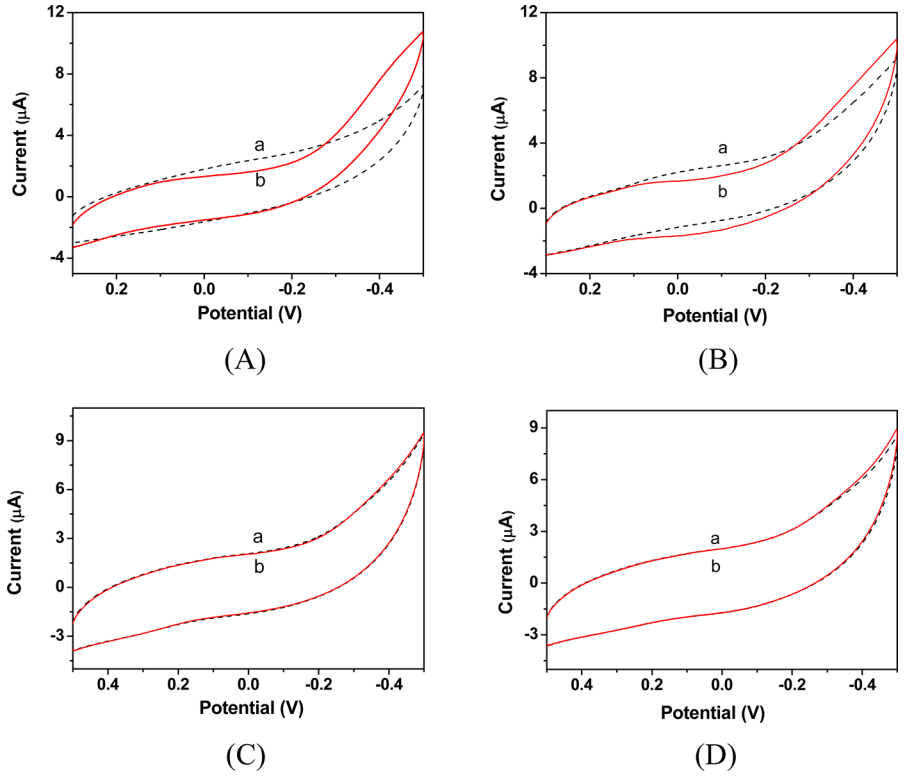

Figure 5. Cyclic voltammograms of the CuMOF-Tyr-Chit/GCE biosensor for responsive(BPF and BPE) and unresponsive BPs (BPS and TBBPA) before (curve b, red solid line) and after the addition of 3 μM bisphenols (curve a, black dashed line): (A) BPF, (B) BPE, (C) BPS, and (D) TBBPA. Scan rate: 0.1 V/s.

DOI: 10.1021/acsami.6b05008
ACS Appl. Mater. Interfaces 2016, 8, 16533−16539

electrochemical response of different BPs on the tyrosinase biosensor is affected not only by the molecular structure, especially the available ortho positions of phenolic hydroxyl groups, but also by the properties of the substituent group (electron acceptor or electron donor) on the bisphenol framework. The electronic cloud distribution of the phenolic hydroxyl groups, which is affected by the substituent group (electron acceptor or electron donor), determines whether the available ortho positions of phenolic hydroxyl groups can be oxidized by the tyrosinase biosensor. As far as we know, this is the first systematic investigation on the electrochemical response characteristics and mechanisms of different BPs on fabricated tyrosinase biosensors. These response mechanisms and general rules are of great significance because they can be used for predicting the response characteristics of many bisphenols and their various derivatives and metabolites on biosensors.

3.3. Anti-Interference Test of the Biosensor for Heavy Metal Ions. Besides for BPs, the potential of the biosensor for analysis of complex environmental samples such as wastewater samples was also explored. In our previous studies, we tested the effect of some organic chemicals on the nanosensor response. The experimental results show that some common organic chemicals (such as acetone, ethanol, methanol, and acetonitrile) have no influence on the performance of the biosensor.[23] Because environmental water samples are extremely complex, usually containing heavy metal ions, the response behavior of the CuMOF-based biosensor for heavy metal ions was evaluated. Heavy metal ions are a major and common enzyme inhibitor, and many reviews have summarized their inhibiting effect and toxicity.[32,33] The biosensor was immersed in high-concentration heavy metal ion buffer solutions (0.1 mM) for 0.5 h, and the remaining tyrosinase biosensor sensitivity after treatment with heavy metal ions was estimated. It was interesting to find that heavy metal ions, which generally inhibit enzyme activity, had little influence on the performance of the fabricated tyrosinase biosensor. The remaining percentage of biosensor sensitivity (S_p) after treatment with 0.1 mM heavy metal ions Hg^{2+}, Pd^{2+}, Cu^{2+}, Fe^{2+}, Co^{2+}, Ba^{2+}, Zn^{2+}, Cd^{2+}, and Ni^{2+} was 81.78, 83.60, 85.24, 88.37, 88.80, 88.70, 93.56, 97.55, and 98.74%, respectively. This means that the sensitivity of this CuMOF-Tyr-Chit/GCE biosensor is almost not affected by these toxic heavy metal ions. The results suggest that this CuMOF-Tyr-Chit/GCE biosensor is also a promising tool for the detection of phenolic pollutants in industrial wastewater, including those metallurgical wastewaters containing high concentrations of heavy metal ions. The good anti-interference ability of the biosensor for heavy metal ions is ascribed to the following reasons. First, the biopolymer chitosan in the CuMOF-chitosan nanocomposite plays a key role in the good anti-interference ability of the biosensor, as chitosan film possesses outstanding film-forming ability and extraordinary adsorption behavior toward various toxic heavy metal ions,[34,35] which eliminates the inhibiting activity of heavy metal ions on tyrosinase molecules. Second, nanoporous CuMOF also contributed to the good anti-interference ability of the biosensor. Ultrastable CuMOF possesses a nanoporous 3D structure with a pore size distribution peak at ~4.9 Å. Although some small ions (such as H^+) can easily pass through these nanopores, those large hydrated heavy metal ions have difficulty diffusing through the nanopores of CuMOF. This study reveals that the CuMOF-chitosan nanocomposite offers an excellent biosensing platform for the construction of diverse biosensors (e.g., enzymes and microbes) for selective detection of targets (e.g., phenolic chemicals in wastewater) even in the presence of high concentrations of heavy metal ions.

4. CONCLUSIONS

In summary, the electrochemical response characteristics and mechanisms of nine kinds of BPs on a CuMOFs-based tyrosinase biosensor was investigated and discussed for the first time. The prepared CuMOFs exhibited a large surface area for tyrosinase immobilization and BP enrichment. It is interesting to note that the developed tyrosinase biosensor showed sensitive responses to BPE, BPF, BPA, BPB, and BPZ, and the response sensitivities were highly dependent on their respective log K_{ow} values. However, the biosensor showed no response to BPS, BPAF, BPAP, or TBBPA, although both BPS, BPAF, and BPAP have structures similar to those of the responsive BPs. The obtained results suggest the electrochemical response of different BPs on tyrosinase biosensor is affected not only by the molecular structure, especially the available ortho positions of phenolic hydroxyl groups, but also by the substituent group properties (electron acceptor or electron donor) on the bisphenol framework. The electronic cloud distribution of the phenolic hydroxyl groups, which is affected by the substituent group (electron acceptor or electron donor), determines whether the available ortho positions of phenolic hydroxyl groups can be oxidized by the tyrosinase biosensor. These response mechanisms and general rules are of great significance because they can be used for predicting the response characteristics of many bisphenols and their various derivatives and metabolites. Owing to the excellent anti-interference ability to heavy metal ions, the CuMOF-chitosan nanocomposite proves to be a promising biosensing platform for the construction of diverse biosensors for selective detection of targets even in the presence of high concentrations of heavy metal ions.

AUTHOR INFORMATION

Corresponding Authors

*E-mail: xianbolu@dicp.ac.cn.

*E-mail: chenjp@dicp.ac.cn.

Author Contributions

‖X.L. and X.W. contributed equally to this work.

Notes

The authors declare no competing financial interest.

ACKNOWLEDGMENTS

This work was supported by the National Natural Science Foundation of China (Grant 21577139), the Youth Innovation Promotion Association, CAS (Grant 2060303), the Science and Technology Service Network Program, CAS (Grant KFJ-EW-STS-099), and the Special Fund for Agro-scientific Research in the Public Interest (Grant 201503108)) and the Fundamental Research Funds for the Central Universities.

REFERENCES

(1) Peretz, J.; Vrooman, L.; Ricke, W. A.; Hunt, P. A.; Ehrlich, S.; Hauser, R.; Padmanabhan, V.; Taylor, H. S.; Swan, S. H.; VandeVoort, C. A.; Flaws, J. A. Bisphenol A and Reproductive Health: Update of Experimental and Human Evidence, 2007−2013. *Environ. Health Perspect.* **2014**, *122* (8), 775−786.

(2) Michalowicz, J. Bisphenol A - Sources, Toxicity and Biotransformation. *Environ. Toxicol. Pharmacol.* **2014**, *37* (2), 738−758.

DOI: 10.1021/acsami.6b05008
ACS Appl. Mater. Interfaces 2016, 8, 16533−16539

(3) Rezg, R.; El-Fazaa, S.; Gharbi, N.; Mornagui, B. Bisphenol A and Human Chronic Diseases: Current Evidences, Possible Mechanisms, and Future Perspectives. *Environ. Int.* **2014**, *64*, 83−90.
(4) Rochester, J. R. Bisphenol A and Human Health: A Review of the Literature. *Reprod. Toxicol.* **2013**, *42*, 132−155.
(5) Suzuki, M.; Sugiyama, T.; Musashi, E.; Kobiyama, Y.; Kashiwada, A.; Matsuda, K.; Yamada, K. Use of Chitosan for Removal of Bisphenol A and Bisphenol Derivatives Through Tyrosinase-Catalyzed Quinone Oxidation. *J. Appl. Polym. Sci.* **2010**, *118* (2), 721−732.
(6) Chen, M. Y.; Ike, M.; Fujita, M. Acute Toxicity, Mutagenicity, and Estrogenicity of Bisphenol-A and Other Bisphenols. *Environ. Toxicol.* **2002**, *17* (1), 80−86.
(7) Yang, Y. J.; Lu, L. B.; Zhang, J.; Yang, Y.; Wu, Y. N.; Shao, B. Simultaneous Determination of Seven Bisphenols in Environmental Water and Solid Samples by Liquid Chromatography-Electrospray Tandem Mass Spectrometry. *J. Chromatogr. A* **2014**, *1328*, 26−34.
(8) Oca, M. L.; Sarabia, L. A.; Herrero, A.; Ortiz, M. C. Optimum pH for the Determination of Bisphenols and Their Corresponding Diglycidyl Ethers by Gas Chromatography-Mass Spectrometry. Migration Kinetics of Bisphenol A from Polycarbonate Glasses. *J. Chromatogr. A* **2014**, *1360*, 23−38.
(9) Caballero-Casero, N.; Lunar, L.; Rubio, S. Analytical Methods for the Determination of Mixtures of Bisphenols and Derivatives in Human and Environmental Exposure Sources and Biological Fluids. A Review. *Anal. Chim. Acta* **2016**, *908*, 22−53.
(10) Ragavan, K. V.; Rastogi, N. K.; Thakur, M. S. Sensors and Biosensors for Analysis of Bisphenol-A. *TrAC, Trends Anal. Chem.* **2013**, *52*, 248−260.
(11) Qu, Y.; Ma, M.; Wang, Z. G.; Zhan, G. Q.; Li, B. H.; Wang, X.; Fang, H. F.; Zhang, H. J.; Li, C. Y. Sensitive Amperometric Biosensor for Phenolic Compounds Based on Graphene-Silk Peptide/Tyrosinase Composite Nanointerface. *Biosens. Bioelectron.* **2013**, *44*, 85−88.
(12) Wu, L. D.; Deng, D. H.; Jin, J.; Lu, X. B.; Chen, J. P. Nano-Graphene-Based Tyrosinase Biosensor for Rapid Detection of Bisphenol A. *Biosens. Bioelectron.* **2012**, *35* (1), 193−199.
(13) Han, M.; Qu, Y.; Chen, S. Q.; Wang, Y. L.; Zhang, Z.; Ma, M.; Wang, Z. G.; Zhan, G. Q.; Li, C. Y. Amperometric Biosensor for Bisphenol A Based on a Glassy Carbon Electrode Modified with a Nanocomposite Made from Polylysine, Single Walled Carbon Nanotubes and Tyrosinase. *Microchim. Acta* **2013**, *180* (11−12), 989−996.
(14) Wang, N.; Zhao, H. Y.; Ji, X. P.; Li, X. R.; Wang, B. B. Gold Nanoparticles-Enhanced Bisphenol A Electrochemical Biosensor Based on Tyrosinase Immobilized onto Self-Assembled Monolayers-Modified Gold Electrode. *Chin. Chem. Lett.* **2014**, *25* (5), 720−722.
(15) Zhou, H. C.; Kitagawa, S. Metal-Organic Frameworks (MOFs). *Chem. Soc. Rev.* **2014**, *43* (16), 5415−5418.
(16) Li, J. R.; Kuppler, R. J.; Zhou, H. C. Selective Gas Adsorption and Separation in Metal-Organic Frameworks. *Chem. Soc. Rev.* **2009**, *38* (5), 1477−1504.
(17) He, Y. B.; Zhou, W.; Qian, G. D.; Chen, B. L. Methane Storage in Metal-Organic Frameworks. *Chem. Soc. Rev.* **2014**, *43* (16), 5657−5678.
(18) Van de Voorde, B.; Bueken, B.; Denayer, J.; De Vos, D. Adsorptive Separation on Metal-Organic Frameworks in the Liquid Phase. *Chem. Soc. Rev.* **2014**, *43* (16), 5766−5788.
(19) Liu, J. W.; Chen, L. F.; Cui, H.; Zhang, J. Y.; Zhang, L.; Su, C. Y. Applications of Metal-Organic Frameworks in Heterogeneous Supramolecular Catalysis. *Chem. Soc. Rev.* **2014**, *43* (16), 6011−6061.
(20) Hu, Z. C.; Deibert, B. J.; Li, J. Luminescent Metal-Organic Frameworks for Chemical Sensing and Explosive Detection. *Chem. Soc. Rev.* **2014**, *43* (16), 5815−5840.
(21) Fu, Y. C.; Li, P. H.; Bu, L. J.; Wang, T.; Xie, Q. J.; Chen, J. H.; Yao, S. Z. Exploiting Metal-Organic Coordination Polymers as Highly Efficient Immobilization Matrixes of Enzymes for Sensitive Electrochemical Biosensing. *Anal. Chem.* **2011**, *83* (17), 6511−6517.
(22) Ma, W. J.; Jiang, Q.; Yu, P.; Yang, L. F.; Mao, L. Q. Zeolitic Imidazolate Framework-Based Electrochemical Biosensor for in Vivo Electrochemical Measurements. *Anal. Chem.* **2013**, *85* (15), 7550−7557.
(23) Wang, X.; Lu, X. B.; Wu, L. D.; Chen, J. P. 3D Metal-Organic Framework as Highly Efficient Biosensing Platform for Ultrasensitive and Rapid Detection of Bisphenol A. *Biosens. Bioelectron.* **2015**, *65*, 295−301.
(24) Yang, Z. J.; Huang, X. C.; Zhang, R. C.; Li, J.; Xu, Q.; Hu, X. Y. Novel Urchin-like In_2O_3-Chitosan Modified Electrode for Direct Electrochemistry of Glucose Oxidase and Biosensing. *Electrochim. Acta* **2012**, *70*, 325−330.
(25) Liu, X. J.; Luo, L. Q.; Ding, Y. P.; Xu, Y. H. Amperometric Biosensors Based on Alumina Nanoparticles-Chitosan-Horseradish Peroxidase Nanobiocomposites for the Determination of Phenolic Compounds. *Analyst* **2011**, *136* (4), 696−701.
(26) Lu, L. M.; Zhang, L.; Zhang, X. B.; Huan, S. Y.; Shen, G. L.; Yu, R. Q. A Novel Tyrosinase Biosensor Based on Hydroxyapatite-Chitosan Nanocomposite for the Detection of Phenolic Compounds. *Anal. Chim. Acta* **2010**, *665* (2), 146−151.
(27) Lee, J. Y.; Olson, D. H.; Pan, L.; Emge, T. J.; Li, J. Microporous Metal-Organic Frameworks with High Gas Sorption and Separation Capacity. *Adv. Funct. Mater.* **2007**, *17* (8), 1255−1262.
(28) Andreescu, S.; Sadik, O. A. Correlation of Analyte Structures With Biosensor Responses Using the Detection of Phenolic Estrogens as a Model. *Anal. Chem.* **2004**, *76* (3), 552−560.
(29) Hu, Y. L.; Huang, Z. L.; Liao, J.; Li, G. K. Chemical Bonding Approach for Fabrication of Hybrid Magnetic Metal-Organic Framework-5: High Efficient Adsorbents for Magnetic Enrichment of Trace Analytes. *Anal. Chem.* **2013**, *85* (14), 6885−6893.
(30) Cui, X. Y.; Gu, Z. Y.; Jiang, D. Q.; Li, Y.; Wang, H. F.; Yan, X. P. In Situ Hydrothermal Growth of Metal-Organic Framework 199 Films on Stainless Steel Fibers for Solid-Phase Microextraction of Gaseous Benzene Homologues. *Anal. Chem.* **2009**, *81* (23), 9771−9777.
(31) Olivares, C.; Solano, F. New Insights into the Active Site Structure and Catalytic Mechanism of Tyrosinase and Its Related Proteins. *Pigm. Cell Melanoma Res.* **2009**, *22* (6), 750−760.
(32) Upadhyay, L. S. B.; Verma, N. Enzyme Inhibition Based Biosensors: A Review. *Anal. Lett.* **2013**, *46* (2), 225−241.
(33) Turdean, G. L. Design and Development of Biosensors for the Detection of Heavy Metal Toxicity. *Int. J. Electrochem.* **2011**, *2011*, 1−15.
(34) Liu, B. J.; Wang, D. F.; Yu, G. L.; Meng, X. H. Adsorption of Heavy Metal Ions, Dyes and Proteins by Chitosan Composites and Derivatives - A Review. *J. Ocean Univ. China* **2013**, *12* (3), 500−508.
(35) Zhang, L.; Zeng, Y. X.; Cheng, Z. J. Removal of Heavy Metal Ions Using Chitosan and Modified Chitosan: A Review. *J. Mol. Liq.* **2016**, *214*, 175−191.

DOI: 10.1021/acsami.6b05008
ACS Appl. Mater. Interfaces 2016, 8, 16533−16539